Journal Pre-proof

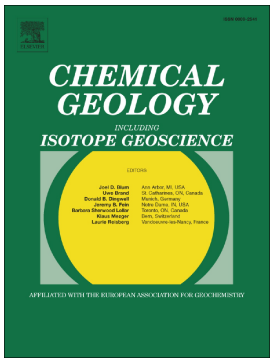

The trace-element composition of a polish stalagmite: Implications for the use of speleothems as a record of explosive volcanism

Alice R. Paine, James U.L. Baldini, Fabian B. Wadsworth, Franziska A. Lechleitner, Robert A. Jamieson, Lisa M. Baldini, Richard J. Brown, Wolfgang Müller, Helena Hercman, Michał Gąsiorowski, Krzysztof Stefaniak, Paweł Socha, Artur Sobczyk, Marek Kasprzak

PII: S0009-2541(21)00101-7

DOI: https://doi.org/10.1016/j.chemgeo.2021.120157

Reference: CHEMGE 120157

To appear in: *Chemical Geology*

Received date: 4 September 2020

Revised date: 28 February 2021

Accepted date: 3 March 2021

Please cite this article as: A.R. Paine, J.U.L. Baldini, F.B. Wadsworth, et al., The trace-element composition of a polish stalagmite: Implications for the use of speleothems as a record of explosive volcanism, *Chemical Geology* (2021), https://doi.org/10.1016/j.chemgeo.2021.120157

This is a PDF file of an article that has undergone enhancements after acceptance, such as the addition of a cover page and metadata, and formatting for readability, but it is not yet the definitive version of record. This version will undergo additional copyediting, typesetting and review before it is published in its final form, but we are providing this version to give early visibility of the article. Please note that, during the production process, errors may be discovered which could affect the content, and all legal disclaimers that apply to the journal pertain.

© 2021 Published by Elsevier.

Journal Pre-proof

The trace-element composition of a Polish stalagmite: Implications for the use of speleothems as a record of explosive volcanism

Alice R. Paine[1,*], James U. L. Baldini[1], Fabian B. Wadsworth[1], Franziska A. Lechleitner[2], Robert A. Jamieson[3], Lisa M. Baldini[4], Richard J. Brown[1], Wolfgang Müller[5], Helena Hercman[6], Michał Gąsiorowski[6], Krzysztof Stefaniak[7], Paweł Socha[7], Artur Sobczyk[8], Marek Kasprzak[9]

[1] Department of Earth Sciences, Durham University, UK, DH1 3LE

[2] Department of Chemistry and Biochemistry and Oeschger Centre for Climate Change Research, University of Bern, Bern, Switzerland

[3] School of Earth and Environment, University of Leeds, UK

[4] School of Health and Life Sciences, Teesside University, UK

[5] Institut für Geowissenschaften, Goethe Universität, Germany

[6] Institute of Geological Sciences, Polish Academy of Sciences, Poland

[7] Department of Palaeozoology, Zoological Institute, University of Wrocław, Poland

[8] Department of Structural Geology and Geological Mapping, Institute of Geological Sciences, University of Wrocław, Poland

[9] Institute of Geography and Regional Development, University of Wrocław, Poland

**currently at the Department of Earth Sciences, University of Oxford, UK, OX1 3AN (alice.paine@earth.ox.ac.uk)*

Journal Pre-proof

Abstract

Identification of volcanic signals preserved in paleoenvironmental records can provide key insights into the timing and consequences of explosive volcanism. Yet the eruption record is incomplete and this confounds our ability to link volcanic eruptions to their impacts on climate and environments. Studies have suggested that stalagmite records can help to address these gaps, through the identification of transient geochemical variability associated with incorporation of elements derived from erupted material. However, the utility of stalagmites for tracing volcanism is poorly constrained globally. Here, we present a high-resolution geochemical dataset for stalagmite NIED08-05 sampled in Niedźwiedzia Cave (Poland). We do this with two primary aims: (1) to test the suitability of NIED08-05 as a record of volcanism since 3 ka BP, and (2) to ascertain whether stalagmites grown in temperate regions preserve volcanic signals with success comparable to those grown in tropical regions. We find transient enrichments of 16 trace elements and the rare-earth-elements Y, La, Nd, which coincide with the timing of some known eruption events. Using Principal Component Analysis (PCA) we find that elements atypically incorporated into calcite (e.g., Fe) co-vary. Similarly, filtering PC1 (17% of the dataset variability) for high magnitude deviations from a baseline signal yields tentative agreement between PC scores and some known large eruptions with tephra found in Poland. We use our analysis to discuss the complexities involved in associating volcanic signals with stalagmite chemistry in temperate regions far from the source of large eruptions. The transport

pathway from volcanic source to stalagmite growth surfaces includes the complex Niedźwiedzia Cave hydrological system and is influenced by dense forest above the cave site. Together these factors increase the potential for attenuation of volcanic-derived chemical signals prior to reaching the stalagmite, and so make it difficult to unambiguously link trace element enrichments in NIED08-05 to volcanic eruptions. Our results provide strong evidence that in a temperate depositional environment far from active volcanoes, climate and hydrology conspire to mute the strength of volcanic geochemical signals. Therefore, this work provides important incentives for future research in this area by highlighting that stalagmites grown in a comparatively simple hydrological regime and grown in caves overlain by thin vegetation cover (such as in tropical regions), may preserve volcanic signatures with greater success than those grown in temperate environments.

Key Words - volcanic eruptions; LA-ICP-MS; principal component analysis; tephra; Holocene; geochemistry

1. Introduction

The impacts of volcanic eruptions can be spatially and temporally extensive (Kobashi et al. 2017; Sigl et al. 2015; Stoffel et al. 2015). Distal transport of volcanic ash (tephra) can cause inter-continental social, political and economic disruption, and atmospheric injection of volcanic gases can cause global climatological perturbation on annual-to-centennial timescales (e.g., Baldini et al. 2018; Zanchettin et al. 2014; Miller et al. 2012; Zhong et al. 2011). Therefore, studying the frequency of past, very large volcanic eruptions is critically important to prepare for future events.

Historical records of volcanism are spatiotemporally limited (Rougier et al. 2018), and therefore the global eruption record largely rely on well-preserved deposits proximal to an eruptive centre. While proximal records can be supplemented by distal tephra, distal deposits are often poorly or transiently preserved. Sulfate spikes associated with eruptions and preserved in ice cores are a primary source of additional information, and can be dated with sub-decadal precision (Sigl et al. 2015; Zielinski et al. 1996). However, adequately resolved polar ice cores reflect a preservation bias toward high-latitude eruptions (Hildreth & Fierstein, 2012). Therefore, many low-latitude eruption signals are missing from the record (e.g., Svensson et al. 2020). Non-polar ice records are limited to high altitude environments where volcanic aerosols are poorly preserved within the ice (Watanabe et al. 2004). Sedimentary sequences found in the low/mid latitudes are also suitable archives of past volcanism (Lowe, 2011), capable of retaining evidence for the timing and frequency of past eruptions by preservation of visible and/or microscopic cryptotephra layers (Lane et al. 2014). If accurately dated, these layers can act as event-stratigraphic markers and can thus provide evidence for past eruption frequency, intensity, plume trajectory, and environmental impacts (Dugmore et al. 2020; Plunkett &

Pilcher, 2018; Watson et al. 2017; Davies et al. 2010; Gale, 2009). However, structural (Payne & Gehrels, 2010), hydrological (Watson et al. 2016, 2015) and anthropogenic (Swindles et al. 2013) disturbances can all alter, remove, or obscure any contained tephra layers, thus confounding their clear detection.

Speleothems (stalactites and stalagmites) are increasingly used as additional archives for eruption chronology and for understanding climate impacts of eruptions. Stalagmite growth is sustained by interaction of weakly acidic infiltrating surface water with calcium carbonate bedrock. Typically, this infiltrating water becomes supersaturated with calcite and, once it reaches the cave atmosphere, degasses CO_2 and deposits $CaCO_3$ to form speleothems. A tendency for continuous growth and a low propensity for diagenetic modification (Frisia & Borsato, 2010) means stalagmites can record past climate (e.g., surface temperature, precipitation, air composition, atmospheric circulation) and environmental conditions (e.g., soil bioproductivity, vegetation dynamics; Baldini, 2010., Fairchild & Treble, 2009) and volcanic eruptions (Jamieson et al. 2015; Badertscher et al. 2014; Frisia et al. 2008a,b).

Two principal mechanisms allow tephra from volcanic eruptions to influence speleothem growth (Figure 1). The first is aeolian transport of tephra directly into the cave by ventilation. Dry deposition of particulate matter onto stalagmite growth surfaces or onto the stalactite's 'catchment' on the cave roof, and direct incorporation into the fabric of the crystalline calcite composite during growth (Badertscher et al. 2014), could therefore reflect variations in atmospheric tephra concentration (Dredge et al. 2013). The second mechanism is by deposition of tephra on the Earth's surface above a cave, and subsequent leaching into an aqueous fluid of surface deposits (e.g. volcanogenic salts; Wadsworth et al. 2020) or of constituents of the tephra itself (Maters et al. 2016). Such leaching can result in groundwater carrying a magmatic signal (Delmelle et al. 2018; Maters et al. 2016; Martin et al. 2009). Soluble or leachable fractions dissolve rapidly upon contact with ground and/or rainwater of a given pH (Jones & Gislason, 2008; Witham et al. 2005). If tephra is deposited above a cave, these leached and dissolved fractions are transported into the karst by percolation through fractures and interconnected pore spaces (Wynn et al. 2013; Fairchild & Treble, 2009): either as colloids, solutes, or bound to organic matter (Hartland et al. 2012). If those surface waters become integrated within the dripwater aquifer, entrained volcanogenic material could be eventually deposited onto the stalagmite (e.g., Jamieson et al. 2015; Badertscher et al. 2014).

Geochemical records sourced from stalagmites show potential for detection of explosive volcanism during the Holocene, with successful applications using stalagmites from Belize (Jamieson et al. 2015), Italy (Frisia et al. 2008a) and Turkey (Badertscher et al. 2014). These studies focus on samples grown in tropical environments exhibiting a pronounced wet season. Therefore, it is unclear whether stalagmites grown in temperate regions, characterized by subdued seasonality in rainfall, retain

volcanic-derived signals with similar success. Here we test the case of a stalagmite grown in a temperate region by presenting a high-resolution geochemical record from a stalagmite from Niedźwiedzia Cave in south-west Poland. This represents an excellent opportunity to further test the capacity of stalagmites to detect volcanism because: (1) south-west Poland is moderated by a temperate maritime climate, whereby mean precipitation rarely drops below 20 mm in a given month (Bryś & Bryś, 2010), (2) the cave is distal from any Holocene-active volcanic centres, and (3) the NIED08-05 stalagmite grew deep within the cave and far from the cave entrances where tephra could have made its way in via aeolian transport (Figure 1). Previous studies have already shown that stalagmites can retain records of volcanism at sites with a high degree of rainfall seasonality (Jamieson et al. 2015). This current study further constrains the types of sites that are sensitive to this signal, thereby clarifying whether stalagmites can act as truly global archives for volcanism in all cases.

2. Site description

2.1. Regional climate

The study was conducted at Jaskinia Niedźwiedzia or Bear Cave, near Kletno, SW Poland. For the period 1981-2010, annual mean temperature in Wrocław (100 km to the north of the study site) was 6.4^{o}C (± 3.0^{o}C). Wrocław also holds the longest continuous records of precipitation and air temperature in Poland, beginning in 1791 (Bryś & Bryś, 2010). Based on a 30-year dataset from Wrocław (1980 – 2010) mean monthly precipitation ranges from 27.2 mm (in February) to 84.4 mm (in July) and temperature ranges from -1.4°C (in January) to 18.7°C (in July) (Figure 2b). Precipitation in SW Poland typically results from the interaction of cold, continental air masses from Eastern Europe and warm, maritime air masses from the Atlantic (Piotrowski & Jędruszkiewicz, 2013). The Kleśnica valley in the Eastern Sudetes, where the Niedźwiedzia Cave is located, has a mean annual air temperature of 5.5 °C for 1992–2003 (Piasecki & Sawiński, 2009). The modern cave entrance is located ~670 m higher than Wrocław meteorological station, and local air circulation in the valley alongside annual air temperature inversions are associated with foehn phenomena (Piasecki & Szymanowski 1995).

2.2. Niedźwiedzia Cave

This study utilises the calcite-dominated stalagmite NIED08-05, extracted from the upper cave level of Jaskinia Niedźwiedzia (50°14,068'N, 16°50,558'E; 790 m a.s.l.; Figure 3), 10 m below the surface. Jaskinia Niedźwiedzia is one of the largest cave systems in the Sudetes Mountains (Gąsiorowski et al. 2015), with a depth of >100 m, and a known passage length exceeding 4000 m (Kostka, 2014).

Formed primarily within carbonate rocks, the karst network is comprised of three chamber levels connected by wide open fractures (Kasprzak & Sobczyk, 2017; Sobczyk et al. 2016). The cave is overlain by thick soils punctuated by exposed marble outcrops, and vegetation cover is predominantly beech-spruce forest. The internal cave environment is stable with a mean air temperature (5-6^{o}C) that reflects the multi-annual mean external temperature and a relative humidity of 94-98% (Piasecki & Sawiński, 2009).

3. Methods

3.1. Cave Monitoring

To constrain the transmission of surface waters through the karst and the stalagmite's sensitivity to seasonal surface conditions, the NIED08-05 feeder drip and simultaneous surface precipitation were monitored between April and June 2008 – prior to stalagmite collection. Between May 2009 and June 2010, monthly-integrated NIED08-05 feeder dripwater at two sites along the same fracture (Figure 3c) and contemporaneous surface rainwater were also collected from the site, for measurement of oxygen isotope ratios ($\delta^{18}O$). This was performed to quantify seasonal water transmission in relation to the karst structure, and soil overburden (Baldini et al. 2019; Baldini et al. 2015).

3.2. Chronology

Despite the cave's proximity to economically viable U deposits that prompted mining operations, and the cave's discovery in 1966, stalagmite NIED08-05 is characterised by very low uranium concentrations (Lechleitner et al. 2016). As a result, large uncertainties were associated with the U-Th chronology and an alternative ^{14}C chronological dating technique was established for the stalagmite (Lechleitner et al. 2016). The NIED08-05 ^{14}C chronology suggests the presence of a growth hiatus at 51.2 mm from the top (Figure 4). Dating uncertainty systematically increases with calcite age, with larger uncertainties in the pre-hiatus interval (Lechleitner et al. 2016). To reduce uncertainties and allow for more precise correlations, only the interval 0-3 ka BP above the hiatus was utilised in this study. We follow Lechleitner et al. (2016) and fit an age-depth trend based on the corrections and model therein (Figure 4).

3.3. LA-ICP-MS

Laser-Ablation Inductively-Coupled-Plasma Mass Spectrometry (LA-ICP-MS) is an analytical technique for *in-situ* geochemical and isotope analysis (Petrelli et al. 2016; Ubide et al. 2015). The

measurements for NIED08-05 were made at Royal Holloway University, using a prototype RESOlution M-50 excimer laser-ablation system (193 nm), in conjunction with a two-volume laser-ablation cell (Müller et al. 2009). This cell was coupled to an Agilent 7500ce/cs quadrupole ICP-MS, and measurements were made in two continuous, parallel tracks – track 1 and track 2 – along the cross section of the speleothem (Figure 4) using a 140 x 10 μm laser slit, and a 15 Hz repetition rate (90 mJ laser spot with an estimated average effective measurement spot diameter of 74 μm; Müller et al. 2009). The track positions are given in Figure 4a. Measurements for track 1 were obtained using a 16.7 μm s^{-1} scan speed, and measurements for track 2 using a 10 μm s^{-1} scan speed (Müller et al. 2009). The concentrations of 20 trace elements were analysed selected for their applicability as both volcanic and paleoclimatic proxies. ^{43}Ca was measured throughout all runs as an internal standard. The Iolite software package was used for data reduction, using NIST 612, NIST 619 and MACS3 standards of quantification (Paton et al. 2011). Stable isotopes ^{24}Mg and ^{25}Mg were both measured in NIED08-05. Using the spot diameter (quoted above) we apply a moving arithmetic mean to all raw data with an averaging window of ± 37 μm (half the laser spot size).

We note that track 1 was taken along the principal growth axis of the stalagmite, such that the path direction of the laser track is always perpendicular to the individual stalagmite laminae, whereas track 2 was taken adjacent and slightly off-axis. To check consistency between two laser tracks, we compared Ba concentrations – an element that is compatible in calcite in each track dataset. In Figure 5 we show the results for Ba in both track 1 and track 2 superposed without any further signal processing. Although there is broad agreement with the low-frequency variability in the datasets (the broad humps and troughs are consistent), there are important differences on length scales of interest to this study. For example, we identify several key abrupt changes in Ba concentration that can be identified in both track 1 and track 2. While both datasets agree as to the presence of these changes, they disagree as to the distance window over which they occur. As illustrative examples, in Figure 5 we show 3 such offsets with 500, 600 and 400 μm distance disagreement, respectively. Using the chronology from Figure 4b, offsets of this magnitude would result in time-discrepancies of 7.6-45 years if the chronology was applied blindly to both datasets. While so-called 'wiggle-match' techniques exist for adjusting the off-axis track 2 to agree with track 1, we prefer to use track 1 as measured, and appeal to the observation that track 2 is off-axis as cause to neglect further analysis with that dataset. We note that this is consistent with the well-reported variation of stalagmite chemistry as a function of distance from the principal growth axis (Vanghi et al. 2019). Therefore, we argue that the general agreement of the low-frequency trends in Ba shown in Figure 5 is evidence of reliability of our measurement protocol, while the apparently subtle offsets in the high-frequency events can be explained by stalagmite geochemical variability off-axis.

3.4. Volcanic eruption selection

Data for Northern Hemisphere eruptions were downloaded from the Large Magnitude Explosive Volcanic Eruptions (LaMEVE) database (Crosweller et al. 2012). We did not include eruptions with a magnitude of less than 4, as Niedźwiedzia Cave is not within 100 km of a volcanic system that has been active in the last 3 ka. So, it is reasonable to assume deposition of any volcanic material at the cave site was limited to fine-grained distal tephra produced during explosive events; which we arbitrarily constrain by defining magnitude 4.0 as a minimum eruption size (Cashman & Rust, 2020).

The database contains a large number of eruptions within a magnitude range of 4.0 – 8.0, all occurring across our interval of interest (Figure 6). Due to the low number of tephrochronological studies undertaken in Poland, we could not confidently determine whether many of these eruptions did deposit tephra over the Niedźwiedzia Cave site. Therefore, we focus on eruptions whose deposits have previously been identified in Polish sediments, (Kinder et al. 2020., Watson et al. 2017; Wulf et al. 2016), which represent good candidates for detection using our technique. These are: Askja1875 (Askja volcano, Iceland; 1875 CE), and AD860B (Mount Churchill, Alaska, USA; 847±1 CE); the latter is at present the only trans-Atlantic eruption with confirmed tephra distribution over Poland (Kinder et al. 2020., Watson et al. 2017).

We also include the Glen Garry isochron (2265±12 BCE), with data sourced from the NEVA database (Swindles et al. 2017). This isochron was identified in Polish sediments by Kinder et al. (2020), however has been further detected in the U.K., Germany, and Scandinavia, suggesting the widespread distribution of tephra from a single eruptive event (Lawson et al. 2012). Kinder et al. (2020) also make tentative correlations between glass shards found in Lake Żabińskie, northeast Poland, and Furnas volcano (Azores). However, the eruptive event during which this tephra was produced is unclear, and hence we do not include the Furnas isochron in our discussion.

3.5. Principal Component Analysis

Principal Component Analysis (PCA) is a dimension-reduction data analysis method which combines the intra-variable association, data dispersion direction and relative importance of these directions in order to assess which Principal Component (PC) explains the largest sum of variability in a multivariate dataset, for which PC1 is the greatest (Abdi & Williams, 2010). Previous application of PCA to a tropical stalagmite facilitated identification of short-lived enrichments temporally coincident with dispersal of tephra over Actun Tunichil Muknal cave, Belize (Jamieson et al. 2015), suggesting this technique can aid detection of volcanic signals within large, high resolution trace element datasets obtained from tropical stalagmites.

To distinguish any distinct modes of trace element variability potentially indicative of volcanic material deposition in NIED08-05, and subsequently test the suitability of PCA for detection of volcanism in a non-tropical, prehistoric archive, we applied PCA to the dataset obtained from NIED08-05. Z-scores were calculated prior to analysis to lessen analysis sensitivity to individual variables. The MATLAB™ *pca* function (MathWorks, 2019) was used to extract coefficients, percentage-variance and PC scores from the dataset. Scores were then plotted as a time-series, to identify discrete signals resulting from increased trace element input to the stalagmite.

4. Results

All elements measured in NIED08-05 have a relatively low background concentration with occasional, short-lived excursions to higher concentrations. This result is similar to many previous LA-ICP-MS analyses of stalagmites and suggests that the excursions in the elemental composition of the stalagmite could be triggered by a short-lived event; in which the water feeding calcite growth is transiently contaminated before returned to 'normal' levels. Here, we report the results of the comparisons between the timing of the element excursions, and the timing of select eruptions with known tephra deposition in Poland.

4.1. Does the stalagmite geochemistry record volcanism?

We focus our analysis on the elements Mg, Sr, Ba, P, Fe, Cu, Pb, I, U, Zn, Al, Mn, Co, Cu, Rb, V, and the rare earth elements (REEs) measured along track 1 in the stalagmite. In Figure 7, we compare variations of these trace elements. The spatial distance along the track is converted to a time axis via the chronology in Figure 4, and we also show the timing of the 3 selected volcanic eruptions for comparison.

Taking into account the uncertainty on the eruption dates, and on the chronology presented here, we see spikes in geochemical concentrations in certain elements apparently coincident with the eruption timing: of (1) the eruption of Mount Churchill at 847±1 CE, and (2) the Glen Garry isochron dated to 226±122 BCE. However, similar coincidences are not seen in concurrence with the eruption of Askja volcano at 1875 CE. It is not clear that the same elements show an enrichment within uncertainty of both (1) and (2); for example, while the eruption of Mount Churchill is coincident with an enrichment in Mn, Cu, P, Rb, Mg, and I, the Glen Garry isochron date is within uncertainty of Mg, Al, Pb, Th, Mn, Cu, Fe, Rb, Co, and the aggregated REE signal. From this, we can see that a greater number of trace element enrichments coincide with Glen Garry – however this is likely a product of greater date uncertainty (yielding a greater range in potential deposition dates), rather than evidence for tephra deposition over Niedźwiedzia Cave.

The absence of a clear match between trace element spikes and an eruption is particularly evident when comparing geochemical signals that fall within uncertainty of the 1875 CE eruption of Askja volcano. The eruption ejected 0.3 km^3 (DRE) rhyolitic tephra along an extended south-eastern dispersal axis (Carey et al. 2010), resulting in widespread transmission into mainland Europe and Scandinavia (Kalliokoski et al. 2020). However, trace element concentrations in NIED08-05 during this eruption do not increase above background levels around the timing of the eruption.

4.2. Principal Component Analysis

Following Jamieson et al. (2015), we apply PCA to the entire LA-ICP-MS dataset. PC1 represents the greatest variability in NIED08-05, accounting for 17% of trace element variability. In Figure 8 we show the PC1 dataset as a time series. PC1 coefficients for trace elements demonstrate co-variance of elements atypically incorporated into calcite, such as the trace Al, Mn, Cu, Zn, Rb, and Fe.

We term the PC1 amplitude in Figure 8a y_1. We use a moving average (centrally-weighted) of 75 year window size – which we term y_s –in order to capture the low-frequency background oscillation in PC1 (Figure 8a). A baseline normalised dataset is therefore $y_T = y_1 - y_s$, where y_T shows the high frequency signal relative to the low-frequency variation (Figure 8b). This is a method by which we can better identify coincidence between a high frequency PC1 signal, and the timing of a known eruption. In Figure 8c & 8d we have applied a threshold such that we only show the peaks that have a magnitude $y_T > 3$, and $y_T > 4$, respectively. These are threshold magnitudes selected based on the hypothesis that the eruption might be recorded in this stalagmite. Note that the Mount Churchill eruption coincides with a peak when $y_T > 3$, but not when $y_T > 4$ (Figure 8c & 8d).

The baseline-normalised and thresholded PC1 scores are given in Figure 8. When $y_T > 3$, these show spikes within uncertainty of the reported timings of (1) the eruption of Mount Churchill at 847±1 CE, and (2) the Glen Garry isochron dated to 226±122 BCE. We also note that, for both eruptions, the raw (non-PCA) elements that were also enriched were captured by this analysis. This could suggest that the elements co-varying within the time-series (thus identified as PC1) also show consistency in certain peaks when cast as PC1 (Figure 8). Nevertheless, as with the data shown in Figure **7**, there is no transient associated PC1 signal with the 1875 CE eruption of Askja, and individual geochemical signals vary between (1) and (2). Due to this inconsistency, we cannot be confident that our geochemical record effectively captures evidence for volcanic eruptions. The mechanisms underpinning this uncertainty form the foundation of our discussion.

5. Discussion

The deposition of trace elements into NIED08-05 appears episodic, and so could represent transient environmental events such as storms or volcanic eruptions. Volcanic material could have reached the NIED08-05 stalagmite by (1) transport of tephra particles into the cave itself by wind and cave-ventilation processes, and/or (2) leaching of tephra from a fall deposit above the cave, and subsequent transport of trace elements in aqueous solution, through the karst to the stalagmite growth surface (Figure 1). However, the presence of such signals cannot be easily deconvolved from processes that may result in take-up or release of these elements in our record, such as karstic and weathering processes. In this section, we discuss the factors that could affect the apparent trace element variability found in NIED08-05. Pertinent to this discussion is the comparison between this stalagmite collected in temperate Poland, and the trace element record found in a stalagmite from Belize grown in tropical conditions (Jamieson et al. 2015). In the latter example (Jamieson et al. 2015), a clear match was established between key eruptions and the trace element variability in that stalagmite, which serves as a key comparison here.

5.1. Does tephra reach Poland?

The mechanisms described above and illustrated in Figure 1 suggest that direct tephra deposition is required to yield a geochemical signal in a given stalagmite record, and that tephra particles would be the dominant carrier of trace elements from a volcanic source to the cave site. Therefore, the first-order control on whether a volcanic eruption can be recorded in the stalagmite record is the propensity for tephra deposition at the cave site.

In recent years, tephrochronological studies have shown that central Europe was regularly impacted by Icelandic volcanism during the Holocene (e.g., Kinder et al. 2020; Watson et al. 2017; Wulf et al. 2016; Housley et al. 2014) as a result of high eruptive frequency, coupled with atmospheric conditions favouring south-eastern dispersal (Lawson et al. 2012). Certain ultra-distal cryptotephras also appear in Central European records (Kinder et al. 2020; Watson et al. 2017), and this extensive dispersal is likely driven by strong unidirectional winds (e.g., Atlantic westerlies in the Northern Hemisphere) and/or jet streams in the Northern Hemisphere (Bursik et al. 2009). However, these meteorological conditions are subject to fluctuations on different spatiotemporal scales, thus the distribution of tephra following an eruption may not follow 'expected' trajectories. For example, geochemical signals in NIED08-05 do not clearly coincide with the timing of the 1875 CE eruption of Askja volcano. Cryptotephras associated with the 1875 CE eruption have been identified in Polish Lakes Żabińskie (Kinder et al. 2020), Tiefer See, Czechowskie (Wulf et al. 2016), and peatland Bagno Kusowo (Watson et al. 2017). The 1875 CE Askja layer is also not the only event from this volcano detected in Central European sediments; others include the early Holocene Askja-S (Wulf et al. 2016), and Glen Garry (Guðmundsdóttir et al. 2016) deposits. Although there is evidence that tephra from the 1875

event was deposited in the Central European region, the absence of coincidence between Askja eruptions and geochemical variability in NIED08-05 could indicate that: (1) tephras were not dispersed so far south following the eruption, and/or (2) only low, undetectable concentrations of tephra reached the cave.

Volcanic eruptions also emit halogens into the atmosphere such as fluorine, chlorine, bromine and iodine (Pyle & Mather, 2009; Aiuppa et al. 2005), which can be removed by adsorption onto the surface of tephra particles. Owing to a high solubility, release of halogen species into the environment may occur more readily via rapid leaching tephra upon contact with ground and surface water (Witham et al. 2005). Here, iodine is the only halogen species within our dataset, and so we examine this element as a potential volcanogenic marker in NIED08-05. However, iodine concentrations do not show any distinct spikes coincident with our selected volcanic eruptions, and instead demonstrate high background concentrations. This suggests that iodine deposition in NIED08-05 is likely not the product of rapid leaching from tephra particles following an eruption. Therefore, providing further evidence that tephra likely did not, in many cases, reach Niedźwiedzia cave.

The dispersal of tephra is a complex problem and depends on the so-called 'volcanic source term' (e.g., Mastin et al. 2009), the meteorological conditions (e.g., Poulidis et al. 2018), and the dynamics in the plume (e.g., secondary effects such as particle aggregation; Brown et al. 2012). Atmospheric circulation impacts tephra areal deposition, and only specific conditions facilitate widespread tephra dispersal. Moreover, airborne tephra concentrations decrease as a function of distance from the source volcano, as particles are removed by sedimentation processes (Green et al. 2016; Rose & Durant, 2009). Therefore, the considerable distance (>2000 km) between Niedźwiedzia Cave and the volcanoes considered in this study could act as a primary control on the presence, or absence, of any eruption signals in our geochemical record.

5.2. Karstic and weathering processes

A second general control on the propagation of volcanic signals through a cave and into a stalagmite record are the processes occurring in the soil and karst transport pathway. Notably the redox state of the soil and karst waters and the provision of water in relation to local precipitation cycles. These processes do not only dictate the ease at which any airborne tephras could reach the stalagmite, but control processes also initiate and drive the leaching of fall deposits above the cave, and the precipitation or dissolution of weathering products. Together these processes can alter the composition of the water that is mobilized and deposited into the stalagmite feeder drip.

5.2.1. Cave ventilation

Based on the morphology of Niedźwiedzia Cave, aeolian transport and dry deposition of airborne volcanic-derived material into the cave appears unlikely. Geomorphological evidence of small open passages in the upper cave levels (Kasprzak & Sobczyk, 2017., Sobczyk et al. 2016), and identification of Pleistocene and Holocene mammal remains within Niedźwiedzia Cave suggest alternative points of cave entry may have existed during the Holocene (Sobczyk et al. 2016., Stefaniak, 2015., Baca et al. 2014). However, NIED08-05 grew deep within the cave which reduces the potential for dry tephra deposition, and there is no evidence of dust deposition within the cave (much of the cave is covered by very clean calcite). Therefore, hydrological routing is the most viable mode of surficial trace element transport and deposition within Niedźwiedzia Cave.

5.2.3. Bedrock dissolution

Dissolution of bedrock commonly affects stalagmite trace element composition caused by prolonged contact between dripwater and host limestone (Jamieson et al. 2016., Rutlidge et al. 2014; Fairchild & Treble, 2009). This can result in variable amounts of prior calcite precipitation (PCP), which is the deposition of calcite from dripwater prior to reaching the stalagmite. This process is enhanced when descending waters can degas more thoroughly, and is responsible for simultaneous elevation of Mg/Ca, Sr/Ca, and Ba/Ca due to the preferential exclusion of Mg/Sr, and Mg/Ba from the calcite lattice (Stoll et al. 2012). NIED08-05 shows weak correlations between Mg and Sr, and Mg and Ba, together with a lack of concurrent Ce enrichment (Drugat et al. 2019) alongside the other REEs (Y, Nd, La), suggesting that PCP is negligible in Niedźwiedzia Cave. Our results support those of Lechleitner et al. (2016), who found a weak correlation between Mg/Ca and $\delta^{13}C$ - suggesting slow degassing of CO_2 from dripwater and subsequently low amounts of PCP.

5.2.3. The hydrological pathway

A primary control on the presence or absence of volcanic signals within the stalagmite is the amount of tephra deposited above the cave. If tephra were deposited above the cave in appreciable amounts, the hydrology of the soil system and Niedźwiedzia system represents a transport pathway through which changes in water chemistry can occur.

The solubility of tephra constituents in groundwater of variable pH can substantially differ, and result in variable and time-lagged pulses of dissolved elements. Fe in tephras demonstrates such variability as the water-soluble mass fraction in tephra is highly variable (Ayris & Delmelle, 2012; Duggen et al. 2010), and so Fe solubility does not correlate with bulk tephra Fe content (Olgun et al. 2011; Jones & Gislason, 2008). This variability confounds the ability to link specific geochemical enrichments to the

composition of glass shards associated with individual eruptions, and thus presents the first challenge of discriminating volcanic signals from those derived from soils.

Once trace elements are leached and chemical constituents enter the ground water, organic ligands would act as a primary complexing agent for particulate and colloidal fractions (Jones & Gislason, 2008); allowing them to be transported into the subsurface aquifer (Hartland et al. 2012). Niedźwiedzia Cave is overlain by dominantly dystric (acidic) cambisols rich in nutrients and organic matter (Panagos et al. 2011; Kabała & Szerszeń, 2002), and proxy reconstructions (Mauri et al. 2015) coupled with meteorological data (Figure 2B., Bryś & Bryś, 2010) suggest a warm and wet Central European climate during the Late Holocene. High saturation of soils due to persistent rainfall at the Niedźwiedzia site would act to not only enhance the bioavailability of trace elements contained in surficial soils, but also increase the concentration of organic ligands upon which trace metals could bind (e.g., Hartland et al. 2012; Borsato et al. 2007; Jones & Gislason, 2008; Kabała & Szerszeń, 2002). This could have enhanced the rate of soil-derived trace element transport and deposition in NIED08-05, meaning trace elements were continuously deposited into the stalagmite throughout the period of growth. Additionally unknown variations in the redox conditions in the waters could result in the precipitation and dissolution of oxyhydroxide compounds, which can take up and release REEs in transient events (e.g. Schreiber et al. 2000).

The importance of organic matter for transport of trace elements into karst systems also links to flow regime. Karst systems dominated by fracture flow (such as Niedźwiedzia) better facilitate the transport of particulates otherwise removed from dripwater by filtration (Hartland et al. 2012), by allowing for high water discharge within the karst. Under these high-flow conditions, Cu, Mn, Pb, Zn, and REEs in both colloidal and particulate form appear more readily mobilized and deposited into speleothems (Tan et al. 2014; Hartland et al. 2012; Zhou et al. 2012, 2008a, b; Borsato et al. 2007). These constituents could include those leached from tephra deposits, but also from soils following flood/waterlogging events.

Taken together, these hydrological processes may represent a key pathway that convolves a volcanic chemical signal with other soil- and karst-based weathering and flow processes, such that deconvolution of those signals is a principal challenge. In turn, this may explain the inconsistency with which we can identify clear associations between our stalagmite record's geochemistry and eruptions known to have deposited tephra in Poland.

6. Comparison with other stalagmite records

We suggest that the reduced fidelity of NIED08-05 as a record of explosive volcanism is linked to four key factors: (1) its distal location relative to active volcanoes, (2) regional climate and hydrology,

(3) depth within the cave, and (4) lack of an extremely precise chronology (especially toward the older sections of the stalagmite). These all serve to complicate the detection of a volcanic signal within the stalagmite. By comparison, the stalagmite ATM-7 from Actun Tunichil Muknal (ATM) cave, Belize, benefits from proximity to active volcanoes, a seasonal climate, a shallow setting, and a very well-constrained chronology (Jamieson et al. 2015) - and therefore records a volcanic-derived geochemical signal.

The seasonality exhibited by the precipitation regime of Belize permits the accumulation of tephra particles on the surface and within the cave (on the cave walls and on the stalagmite) so that when the rainy season begins, this material is flushed to the growing stalagmite. This not only improved the annual rhythm of stalagmite growth, but also limited the influx of surficial trace elements into sub-surface aquifers to a distinct point in time. Therefore, the temporal offset between the eruption date and trace element enrichment in ATM-7 reflects eruption timing relative to the wet season onset; suggesting tephra deposited at the site was retained in the soil/karst until a marked increase in precipitation. No such periodicity exists for NIED08-05, and the stalagmite feeder drip (Figure S1) appears governed by persistent infiltration of surface water, meaning it never ceases completely. Monitoring of the Niedźwiedzia hydrology reveals that not all rain events trigger a drip response (Figure S1a). This suggests that a minimum rainfall accumulation is required before water will infiltrate down into the karst, and into the hydrological system feeding the NIED08-05 drip. Moreover, observed $\delta^{18}O$ variability suggests the NIED08-05 feeder drip preserves a low $\delta^{18}O$ autumn/winter precipitation signal; despite the bulk of precipitation falling during summer (Figures S1 & S2). It is possible that this signal reflects seasonal variations in degassing, with cooler air circulation in winter driving more efficient degassing (Frisia et al. 2003). However, $\delta^{18}O$ signals in NIED08-05 could also suggest that evapotranspiration from the overlying deciduous forest significantly limits summer rainfall infiltration, meaning winter precipitation is able to infiltrate unimpeded, either immediately or as spring meltwater. From this, muted $\delta^{18}O$ variability would suggest drip water is not only reasonably well filtered in the aquifer, but that geochemical enrichments could occur sporadically throughout the year rather than at distinct points in time. This agrees with the complexity exhibited by the NIED08-05 trace element record.

The transport of surficial trace elements would follow a similarly continuous rate of deposition, confounding identification of distinct volcanic-derived geochemical signals. ATM cave has two entrances at different elevations, which facilitates cave ventilation and the ingress of tephra into the cave. Our research, hence, suggests that dry deposition of tephra into the cave is a critical factor, avoiding the complexities associated with the reprocessing and hydrological transport of tephra deposited on a soil.

Finally, high uncertainties (between 0.3 and 3 ka) within the NIED08-05 chronology confound efforts to link short-lived geochemical excursions with short-lived volcanic eruptions, particularly if eruption dates are not well constrained. The ^{14}C chronology used to date trace element enrichments in this study was developed assuming a constant rate of calcite accretion, however this does not account for growth rate variabilities in response to environmental change (Fairchild & Treble, 2009), which may manifest in the NIED08-05 record as distinct strata and/or Mg/Ca excursions (Lechleitner et al. 2016). In contrast, the ATM-7 record benefits from a very low uncertainty chronology ($\pm$1 year) over a recent time interval (the 1980s) covering historical eruptions with no dating uncertainty.

7. Conclusions

The utility of stalagmite records for improving tephrochronological frameworks is appealing because stalagmites can be dated using absolute methods and they are distributed widely in caves across all latitudes. Stalagmite records from Belize (Jamieson et al. 2015), Turkey (Badertscher et al. 2014), and Italy (Frisia et al. 2008) present encouraging evidence that speleothems can retain geochemical evidence of tephra deposition originating from explosive volcanic eruptions. Here, we use a stalagmite from a poorly ventilated site in SW Poland (Niedźwiedzia Cave) to test this method, and our results suggest that not all stalagmite records preserve volcanic signals unambiguously.

This result yields important insights into the criteria necessary for volcanic signal preservation within stalagmites. Principally, stalagmites in close proximity to candidate eruptive vents are most likely to record volcanism. Additionally, comparison between our results and those from stalagmites in tropical climates suggests that the best results would be found for stalagmites sampled from caves that are dynamically ventilated, in climate regions that experience seasonal rainfall patterns, and at drip sites fed by diffuse flows rather than fractures (reducing the likelihood that soil colloidal material is transported by recharge water). Finally, a stalagmite chronology with low uncertainties is critical for confidently linking stalagmite trace element concentration spikes with volcanism.

The stalagmite and site discussed here represent amongst the most challenging conditions for the preservation and extraction of a volcanic signal. We posit that these results will help future studies identify optimal locations for tephrochronological studies using stalagmites. Stalagmites have the potential to fill gaps within tephrochronological frameworks, complementing other more well-established archives. However, our study suggests that not all stalagmites are suitable for this purpose, and our results further constrain the characteristics of cave sites and samples most likely to yield tephrochronological data.

Acknowledgements

This research was supported by a Marie Curie Intra-European Fellowship grant (PIEF-GA-2008-221706) to Lisa M. Baldini. The authors are grateful to the Niedźwiedzia Cave administration for permitting access into the cave for the purpose of scientific research. We also gratefully acknowledge the Volcanic Global Risk Identification and Analysis Project (VOGRIPA) for their provision of open-access eruption data, which was utilised in this study. David Pyle and Francesco Pausata are also thanked for their valuable insights in the early stages of manuscript preparation. We thank our three anonymous reviewers and editor, for their comments, which helped to improve the manuscript.

Journal Pre-proof

References

Abdi, H., Williams, L.J. (2010) Principal component analysis. *Wiley Interdisciplinary Reviews: Computational Statistics* **2**: 433–459

Aiuppa, A., Federico, C., Franco, A., Giudice, G., Gurrieri, S., Inguaggiato, S., Liuzzo, M., McGonigle, A.J.S., and Valenza, M. (2005) Emission of bromine and iodine from Mount Etna volcano. *Geochemistry, Geophysics, Geosystems* **6**: 1–8, doi:10.1029/2005GC000965.

Ayris, P.M., Delmelle, P. (2012) The immediate environmental effects of tephra emission. *Bulletin of Volcanology* **74**: 1905–1936. https://doi.org/10.1007/s00445-012-0654-5

Ayris, P., Delmelle, P. (2012b) Volcanic and atmospheric controls on ash iron solubility: A review. *Physics and Chemistry of the Earth* **45–46**: 103–112. https://doi.org/10.1016/j.pce.2011.04.013

Baca, M., Mackiewicz, P., Stankovic, A., Popović., Stefaniak, K., Czarnogórska, K., Nadachowski, Gąsiorowski, M., Hercman, H., Weglenski, P. (2014) Ancient DNA and dating of cave bear remains from Niedźwiedzia Cave suggest early appearance of *Ursus ingressus* in Sudetes. *Quaternary International* **339-340**: 217-224

Badertscher, S., Borsato, A., Frisia, S., Cheng, H., Edwards, R.L., Tüysüz, O., Fleitmann, D. (2014) Speleothems as sensitive recorders of volcanic eruptions – the Bronze Age Minoan eruption recorded in a stalagmite from Turkey. *Earth and Planetary Science Letters* **392**: 58-66

Baldini, J.U.L. (2010) The geochemistry of cave calcite deposits as a record of past climate. *The Sedimentary Record* **8**(2): 4-9

Baldini, J.U.L., Brown, R.J., McElwaine, J.N. (2015) Was millennial scale climate change during the Last Glacial triggered by explosive volcanism? *Scientific Reports* **5**: 17442

Baldini, L.M., Baldini, J.U.L., McDermott, F., Arias, P., Cueto, M., Fairchild, I.J., Hoffmann, D.L., Mattey, D.P., Müller, W., Nita, D.C., Ontañón, R., Garciá-Moncó, C., Richards, D.A. (2019) North Iberian temperature and rainfall seasonality over the Younger Dryas and Holocene. *Quaternary Science Reviews* **226**: 1-22

Baldini, L.M., McDermott, F., Baldini, J.U.L., Arias, P., Cueto, M., Fairchild, I.J., Hoffman, D.L., Mattey, D.P., Müller, W., Nita, D.C., Ontañón, R., Garciá-Moncó, C., Richards, D.A. (2015) Regional temperature, atmospheric circulation, and sea-ice variability within the Younger Dryas Event constrained using a speleothem from northern Iberia. *Earth and Planetary Science Letters* **419**: 101-110.

Baldini, L.M., McDermott, F., Foley, A.M., Baldini, J.U.L. (2008) Spatial variability in the European winter precipitation d18O-NAO relationship: Implications for reconstructing NAO-mode climate variability in the Holocene. *Geophysical Research Letters* **35**: L04709

Borsato, A., Frisia, S., Wynn, P.M., Fairchild, I.J., Miorandi, R. (2015) Sulphate concentration in cave dripwater and speleothems: long-term trends and overview of its significance as proxy for environmental processes and climate changes. *Quaternary Science Reviews* **127**: 48-60

Brown, R.J., Bonadonna, C., Durant, A.J. (2012) A review of volcanic ash aggregation. *Physics & Chemistry of the Earth* **45-46**: 65-78

Brown, S.K., Crosweller, H.S., Sparks, R.S.J., Cottrell, E., Deligne, N.I., Guerrero, N.O., Hobbs, L., Kiyosugi, K., Loughlin, S.C., Siebert, L., Takarada, S. (2014) Characterisation of the Quaternary eruption record: analysis of the Large Magnitude Explosive Volcanic Eruptions (LaMEVE) database. *Journal of Applied Volcanology* **3**: 5

Bryś, K., Bryś, T. (2010) Reconstruction of the 217-year (1791-2007) Wrocław air temperature and precipitation series. Bulletin of Geography: *Physical Geography Series* **3**: 121-171

Bursik, M.I., Kobs, S.E., Burns, A., Braitseva, O.A., Bazanova, L.I., Melekestsev, I.V., Kurbatov, A., Pieri, D.C. (2009) Volcanic plumes and wind: Jetstream interaction examples and implications for air traffic. *Journal of Volcanology and Geothermal Research* **186**: 60-67

Carey, R. J., Houghton, B.F., Thordarson, T. (2010), Tephra dispersal and eruption dynamics of wet and dry phases of the 1875 eruption of Askja Volcano, Iceland. *Bulletin of Volcanology* **72**: 259–278

Chester, D.K., Duncan, A., Coutinho, R., Wallenstein, N., Branca, S. (2018) Communicating Information on Eruptions and Their Impacts from the Earliest Times Until the Late Twentieth Century. In: *Observing the Volcano World, Advances in Volcanology*: 419-443

Journal Pre-proof

Collister, C., Mattey, D. (2008) Controls on water drop volume at speleothem drip sites: An experimental study. *Journal of Hydrology* **358**: 259-267

Crosweller, H.S., Arora, B., Brown, S.K., Cottrell, E., Deligne, N.I., Guerrero, N.O., Hobbs, L., Kiyosugi, K., Loughlin, S.C., Lowndes, J., Nayembil, M., Siebert, L., Sparks, R. S.J., Takarada, S., Venzke, E. (2012) Global database on large magnitude explosive volcanic eruptions (LaMEVE). *Journal of Applied Volcanology* **1**: 4

Davies, S.M., Larsen, G., Wastegård, S., Turney, C.S.M., Hall, V.A., Coyle, L., Thordarson, T. (2010) Widespread dispersal of Icelandic tephra: how does the Eyjafjöll eruption of 2010 compare to past Icelandic events? *Journal of Quaternary Science* **25**(5): 605-611

Delmelle, P., Wadsworth, F.B., Maters, E.C., Ayris, P.M. (2018) High temperature reactions between gases and ash particles in volcanic eruption plumes. *Reviews in Mineralogy and Geochemistry* **84**(1): 285-308.

Dredge, J., Fairchild, I.J., Harrison, R.M., Fernandez-Cortes, A., Sanchez-Moral, S., Jurado, V., Gunn, J., Smith, A., Spötl, C., Mattey, D., Wynn, P.M., Grassineau, N. (2013) Cave aerosols: distribution and contribution to speleothem geochemistry. *Quaternary Science Reviews* **63**: 23-41

Drugat, L., Pons-Branchu, E., Douville, E., Foliot, L., Bordier, L., Roy-Barman, M. (2019) Rare earth and alkali elements in stalagmites, as markers of Mediterranean environmental changes during Termination I. *Chemical Geology* **525**: 414-423

Dugmore, A. J., Thompson, P.I.J., Streeter, R.T., Cutler, N.A., Newton, A.J., Kirkbride, M.P. (2020) The interpretive value of transformed tephra sequences. *Journal of Quaternary Science* **35**(1): 23-38

Fairchild, I.J., Treble, P.C. (2009) Trace elements in speleothems as recorders of environmental change. *Quaternary Science Reviews* **28**: 449-468

Fohlmeister, J., Lechleitner, F.A. (2019) STAlagmite dating by radiocarbon (star): A software tool for reliable and fast age depth modelling. *Quaternary Geochronology* **51**: 120-129

Frisia, S., Borsato, A., Susini, J. (2008a) Synchrotron radiation applications to past volcanism archived in speleothems: an overview. *Journal of Volcanology and Geothermal Research* **177**: 96-100

Frisia, S., Badertscher, S., Borsato, A., Susini, J., Göktürk, O.M., Cheng, H., Edwards, R.L., Kramers, R.L., Tüysüz, O., Fleitmann, D. (2008b) The use of stalagmite geochemistry to detect past volcanic eruptions and their environmental impacts. *PAGES News* **16**(3): 25-26

Frisia, S., Borsato, A., Fairchild, I.J., Susini, J. (2005) Variations in atmospheric sulphate recorded in stalagmites by synchrotron micro-XRF and XANES analyses. *Earth and Planetary Science Letters* **235**: 729–740.

Frisia, S., Borsato, A., Preto, N., McDermott, F. (2003) Late Holocene annual growth in three Alpine stalagmites records the influence of solar activity and the North Atlantic Oscillation on winter climate. *Earth and Planetary Science Letters* **216**: 411–424

Gąsirowski, M., Hercman, H., Pruszkowska, A., Błaszczyk, M. (2015) Drip rate and tritium activity in the Niedźwiedzia Cave system (Poland) as a tool for tracking water circulation paths and time in karstic systems. *Geochronometria* **42**: 210-216

Green, R.M., Bebbington, M.S., Jones, G., Cronin, S.J., Turner, M.B. (2016) Estimation of tephra volumes from sparse and incompletely observed deposit thicknesses. *Bulletin of Volcanology* **78**: 25

Guðmundsdóttir, E.R., Larsen, G., Björck, S., Ingólfsson, Ó., Striberger, J. (2016) A new high-resolution Holocene tephra stratigraphy in eastern Iceland: Improving the Icelandic and North Atlantic tephrochronology. *Quaternary Science Reviews* **150**: 234–249. https://doi.org/10.1016/j.quascirev.2016.08.011

Hartland, A., Fairchild, I.J., Lead, J.R., Borsato, A., Baker, A., Frisia, S., Baalousha, M. (2012) From soil to cave: transport of trace metals by natural organic matter in karst dripwaters. *Chemical Geology* **304–305**: 68–82

Hildreth, W., Fierstein, J. (2012) Katmai volcanic cluster and the great eruption of 1912. *Geological Society of America Bulletin* **112**: 1594-1620

Holasek, R. E., Self, S., Woods, A.W. (1996) Satellite observations and interpretation of the 1991 Mount Pinatubo eruption plumes. *Journal of Geophysical Research* **101**: 27635– 27655

Jamieson, R. A., Baldini, J. U. L., Brett, M. J., Taylor, J., Ridley, H. E., Ottley, C. J., Prufer, K. M., Wassenburg, J. A., Scholz, D., Breitenbach, S. F. M. (2016) Intra- and inter-annual uranium concentration variability in a Belizean stalagmite controlled by prior aragonite precipitation: a new tool for reconstructing hydro-climate using aragonitic speleothems. *Geochimica et Cosmochimica Acta* **190**: 332–346

Jamieson, R. A., Baldini, J.U.L., Frappier, A.B., Müller, W., (2015) Volcanic ash fall events identified using principal component analysis of a high-resolution speleothem trace element dataset. *Earth & Planetary Science Letters* **426**: 36-45

Jensen, B.J.L., Pyne-O'Donnell, S., Plunkett, G., Froese, D.G., Hughes, P.D.M., Sigl, M., McConnell, J.R., Amesbury, M.J., Blackwell, P.G., van den Bogaard, C., Buck, C.E., Charman, D.J., Clague, J.J., Hall, V.A., Koch, J., Mackay, H., Mallon, G., McColl, L., Pilcher, J.R. (2014) Transatlantic distribution of the Alaskan White River Ash. *Geology* **42**: 875–878

Jones, M.T., Gislason, S.R. (2008) Rapid releases of metal salts and nutrients following the deposition of volcanic ash into aqueous environments. *Geochimica et Cosmochimica Acta* **72**: 3661–3680

Kabała, C., Szerszeń, L. (2002) Profile distributions of lead, zinc, and copper in Dystric Cambisols developed from granite and gneiss of the Sudetes Mountains, Poland. *Water, Air, and Soil Pollution* **138**: 307–317. https://doi.org/10.1023/A:1015591607154

Kalliokoski, M., Guðmundsdóttir, E.R., Wastegård, S. (2020) Hekla 1947, 1845, 1510 and 1158 tephra in Finland: challenges of tracing tephra from moderate eruptions. *Journal of Quaternary Science*: 1-14

Kasprzak, M., Sobczyk, A. (2017) Searching for the void: improving cave detection accuracy by multi-faceted geophysical survey reconciled with LiDAR DTM. *Zeitschrift für Geomorphologie* **61**(2): 45-59

Kobashi, T., Menviel, L., Jeltsch-Thömmes, Vinther, B.M., Box, J.E., Muscheler, R., Nakaegawa, T., Pfister, P.L., Döring, M., Leuenberger, M., Wanner, H., Ohmura, A. (2017) Volcanic influence on centennial to millennial Holocene Greenland temperature change. *Scientific Reports* **7**: 1441

Kostka, S. (2014). Map of the Niedźwiedzia Cave in Kletno (Central Geological Database). Warsaw: Polish Geological Institute. http://jaskiniepolski.pgi.gov.pl/ (Date Accessed: 2/8/2020)

Lane, C.S., Cullen, V., White, D., Bramham-Law, C., Smith, V. (2014) Cryptotephra as a dating and correlation tool in archaeology. *Journal of Archaeological Science* **42**: 42-50

Lawson, I,T., Swindles, G.T., Plunkett, G., Greenberg, D. (2012) The spatial distribution of Holocene cryptotephras in north-west Europe since 7 ka: implications for understanding ash fall events from Icelandic eruptions. *Quaternary Science Reviews* **41**: 57-66

Lechleitner, F.A., Fohlmeister, J., McIntyre, C., Baldini, L.M., Jamieson, R.A., Hercman, H., Gąsiorowski, M., Pawlak, J., Stefaniak, K., Socha, P, Eglinton, T.I., Baldini, J.U.L. (2016) A novel approach for construction of radiocarbon-based chronologies for speleothems. *Quaternary Geochronology* **35**: 54-66

Lowe, D.J. (2011) Tephrochronology and it's application: A review. *Quaternary Geochronology* **6**: 107-153

Martin, R.S., Watt, S.F.L., Pyle, D.M., Mather, T.A., Matthews, N.E., Georg, R.B., Day, J.A., Fairhead, T., Witt, M.L.I., Quayle, B.M. (2009) Environmental effects of ashfall in Argentina from the 2008 Chaitén volcanic eruption. *Journal of Volcanology and Geothermal Research* **184**: 462-472

Mastin, L.G., Guffanti, M., Servranckx, R., Webley, P., Barsotti, S., Dean, K., Durant, A., Ewert, J.W., Neri, A., Rose, W.I., Schneider, D., Siebert, L., Stunder, B., Swanson, G., Tupper, A., Volentik, A., Waythomas, C.F. (2009) A multidisciplinary effort to assign realistic source parameters to models of volcanic ash-cloud transport and dispersion during eruptions. *Journal of Volcanology and Geothermal Research* **186**: 10–21. https://doi.org/10.1016/j.jvolgeores.2009.01.008

Maters, E.C., Delmelle, P., Bonneville, S. (2016) Atmospheric Processing of Volcanic Glass: Effects on Iron Solubility and Redox Speciation. *Environmental Science and Technology* **50**: 5033–5040. https://doi.org/10.1021/acs.est.5b06281

Mauri, A., Davis, B.A.S., Collins, P.M., Kaplan, J.O. (2015) The climate of Europe during the Holocene: A gridded pollen-based reconstruction and its multi-proxy evaluation. *Quaternary Science Reviews* **112**: 109–127. https://doi.org/10.1016/j.quascirev.2015.01.013

Miller, G.H., Geirsdóttir, Á., Zhong, Y., Larsen, D.J., Otto-Bliesner, B.L., Holland, M.M., Bailey, D.A., Refsnider, K.A., Lehman, S.J., Southon, J.R., Anderson, C., Björnsson, H., Thordarson, T. (2012) Abrupt onset of the Little Ice Age triggered by volcanism and sustained by sea-ice/ocean feedbacks. *Geophysical Research Letters* **39**: L02708

Müller, W., Shelley, M., Miller, P., Broude, S. (2009) Initial performance metrics of a new custom-designed ArF excimer LA-ICPMS system coupled to a two-volume laser-ablation cell. *Journal of Analytical Atomic Spectrometry* **24**: 209

Olgun, N., Duggen, S., Croot, P.L., Delmelle, P., Dietze, H., Schacht, U., Óskarsson, N., Siebe, C., Auer, A., Garbe-Schönberg, D. (2011) Surface ocean iron fertilization: The role of airborne volcanic ash from subduction zone and hot spot volcanoes and related iron fluxes into the Pacific Ocean. *Global Biogeochemical Cycles* **25**: 1–15. https://doi.org/10.1029/2009GB003761

Journal Pre-proof

Olgun, N., Duggen, S., Croot, P.L., Delmelle, P., Dietze, H., Schacht, U., Óskarsson, N., Siebe, C., Auer, A., Garbe-Schönberg, D., 2011. Surface ocean iron fertilization: The role of airborne volcanic ash from subduction zone and hot spot volcanoes and related iron fluxes into the Pacific Ocean. *Global Biogeochemical Cycles* **25**: 1–15. https://doi.org/10.1029/2009GB003761

Palais, J.M., Taylor, K., Mayewski, P.A., Grootes, P. (1991) Volcanic ash from the 1362 A.D. Öræfajökull eruption (Iceland) in the Greenland ice sheet. *Geophysical Research Letters* **18**: 1241–1244

Panagos, P., Jones, A., Bosco, C., Senthil Kumar, P.S. (2011) European digital archive on soil maps (EuDASM): Preserving important soil data for public free access. *International Journal of Digital Earth* **4**: 434–443. https://doi.org/10.1080/17538947.2011.596580

Paton, C., Hellstrom, J., Paul, B., Woodhead, J., Hergt, J. (2011) Iolite: freeware for the visualisation and processing of mass spectrometric data. *Journal of Analytical Atomic Spectrometry* **26**: 2508

Payne, R., Gehrels, M. (2010) The formation of tephra layers in peatlands: an experimental approach. *Catena* **81**: 12-23

Petrelli, M., Laeger, K., Perugini, D. (2016) High spatial resolution trace element determination of geological samples üy laser ablation quadrupole plasma mass spectrometry: implications for glass analysis in volcanic products. [Online] https://arxiv.org/ftp/arxiv/papers/1706/1706.10120.pdf (Accessed: 18/11/2019)

Piasecki, J., Sawiński, T. (2009) The Niedźwiedzia Cave in the climatic environment of the Kleśnica Valley (Śnieżnik Massif). In: Stefaniak, K., Tyc, A., Socha, P. (Eds) *Karst of the Częstochowa Upland and of the Eastern Sudetes: palaeoenvironments and protection.* Studies of the Faculty of Earth Sciences, University of Silesia **56**: 423 – 454

Piasecki, J., Szymanowski, M. (1995) Warunki klimatyczne w górnym odcinku doliny Kleśnicy w Masywie Śnieżnika Kłodzkiego (Climatic conditions in the upper section of the Kleśnica valley in the Śnieżnik Kłodzki Massif). Acta Universitatis Wratislaviensis 1705, Prace Instytutu Geograficznego. Ser. C, Meteorologia i Klimatologia 2: 89-106 (in Polish with Eng. abstract)

Plunkett, G., Pilcher, J. R. (2018). Defining the potential source region of volcanic ash in northwest Europe during the mid- to late Holocene. *Earth-Science Reviews* **179**: 20-37

Poulidis, A.P., Phillips, J.C., Renfrew, I.A., Barclay, J., Hogg, A., Jenkins, S.F., Robertson, R., Pyle, D.M. (2018) Meteorological Controls on Local and Regional Volcanic Ash Dispersal. *Scientific Reports* **8**: 1–11. https://doi.org/10.1038/s41598-018-24651-1

Pyle, D.M., Mather, T.A. (2009) Halogens in igneous processes and their fluxes to the atmosphere and oceans from volcanic activity: A review. *Chemical Geology* **263**: 110–121. doi:10.1016/j.chemgeo.2008.11.013.

Pyne O'Donnell, S.D.F., Jensen, B.J.L. (2020) Glacier Peak and mid-Lateglacial Katla cryptotephras in Scotland: potential new intercontinental and marine-terrestrial correlations. Journal fo Quaternary Science 35 (1-2): 155-162

Rose, W.I., Durant, A.J. (2009) Fine ash content of explosive eruptions. *Journal of Volcanology and Geothermal Research* **186**: 32–39. https://doi.org/10.1016/j.jvolgeores.2009.01.010

Rougier, J., Sparks, R.S.J., Cashman, K.V. (2018) Regional and global under-recording of large explosive eruptions in the past 1000 years. *Journal of Applied Volcanology* **7**:1

Rutlidge, H., Baker, A., Marjo, C.E., Andersen, M.S., Graham, P.W., Cuthbert, M.O., Rau, G.C., Roshan, H., Markowska, M., Mariethoz, G., Jex, C.N. (2014) Dripwater organic matter and trace element geochemistry in a semi-arid karst environment: Implications for speleothem paleoclimatology. *Geochimica et Cosmochimica Acta* **135**: 217-230

Schmidt, A., Robock, A. (2015) Volcanism, the atmosphere and climate through time. In: Schmidt, A., Fristad, K., Elkins-Tanton, L. (Eds.) *Volcanism and Global Environmental Change.* Cambridge, Cambridge University Press: 195-207.

Schreiber, M.E., Simo, J.A., Freiberg, P.G. (2000) Stratigraphic and geochemical controls on naturally occurring arsenic in groundwater, eastern Wisconsin, USA. *Hydrogeology Journal* **8**(2): 161-176.

Sigl, M., Winstrup, M., McConnell, J., Welten, K.C., Plunkett, G., Ludlow, F., Büntgen, U., Caffee, M., Chellman, N., Dahl-Jensen, D., Fischer, H., Kipfstuhl, S., Kostick, C., Maselli, O.J., Mekhaldi, F., Mulvaney, R., Muscheler, R., Pasteris, D.R., Pilcher, J.R., Salzer, M., Schüpbach, S., Steffensen, J.P., Vinther, B.M., Woodruff, T.E. (2015) Timing and climate forcing of volcanic eruptions for the past 2500 years. *Nature* **523**: 543-549

Sobczyk, A., Kasprzak, M., Marciszak, A., Stefaniak, K. (2016) Karst phenomena in metamorphic rocks of the Śnieżnik Massif (East Sudetes): state-of-the-art and significance for tracing a Late-Cenozoic evolution of the Sudetes. *Przegląd Geologiczny* **64**(9): 710-718

Stefaniak, K. (2015) Neogene and Quaternary Cervidae from Poland. Institute of Systematics and Evolution of Animals Polish Academy of Sciences, Kraków: 204.

Stoffel, M., Khodri, M., Corona, C., Guillet, S., Poulain, V., Bekki, S., Guiot, J., Luckman, B.H., Oppenheimer, C., Lebas, N., Beniston, M., Masson-Delmotte, V. (2015). Estimates of volcanic-induced cooling in the Northern Hemisphere over the past 1,500 years. *Nature Geoscience* **8**: 784–788

Stoll, H.M., Müller, W., Prieto, M. (2012) I-STAL, a model for interpretation of Mg/Ca, Sr/Ca and Ba/Ca variations in speleothems and its forward and inverse application on seasonal to millennial scales. *Geochemistry, Geophysics, Geosystems* **13**(1): Q09004

Svensson, A., Dahl-Jensen, D., Steffensen, J.P., Blunier, T., Rasmussen, S.O., Vinther, B.M., Vallelonga, P., Capron, E., Gkinis, V., Cook, E., Kjær, H.A., Muscheler, R., Kipfstuhl, S., Wilhelms, F., Stocker, T.F., Fischer, H., Adolphi, F., Erhardt, T., Sigl, M., Landais, A., Parrenin, F., Buizert, C., McConnell, J.R., Severi, M., Mulvaney, R., Bigler, M. (2020) Bipolar volcanic synchronization of abrupt climate change in Greenland and Antarctic ice cores during the last glacial period. *Climate of the Past* **16**: 1565–1580. https://doi.org/10.5194/cp-16-1565-2020

Swindles, G.T., Galloway, J., Outram, Z., Turner, K., Schofield, J.E., Newton, A.J., Dagmore, A.J., Church, M.J., Watson, E.J., Batt, C., Bond, J., Edwards, K.J., Turner, V., Bashford, D. (2013) Re-deposited cryptotephra layers in Holocene peats linked to anthropogenic activity. *Holocene* **23**: 1493-1501

Swindles, G.T., Watson, E.J., Savov, I.P., Cooper, C.L., Lawson, I.T., Schmidt, A., Carrivick, J.L. (2017) Holocene volcanic ash database for Northern Europe: *Database*, doi:10.13140/RG.2.2.11395.50966.

Tan, L., Shen, C.C., Cai, Y., Lo, L., Cheng, H., An, Z. (2014) Trace-element variations in an annually layered stalagmite as recorders of climatic changes and anthropogenic pollution in central China. *Quaternary Research (United States).* **81**: 181–188. https://doi.org/10.1016/j.yqres.2013.12.001

Thordarson, T., Höskuldsson, A. (2008) Postglacial eruptions in Iceland. *Jökull* **58**: 197–228

Ubide, T., McKenna, C.A., Chew, D.M., Kamber, B.S. (2015) High-resolution LA-ICP-MS trace element mapping of igneous minerals: In search of magma histories. *Chemical Geology* **409**: 157-168

Vanghi, V., Borsato, A., Frisia, S., Howard, D.L., Gloy, C., Hellstrom, J., Bajo, P. (2019) High-resolution synchrotron X-ray fluorescence investigation of calcite coralloid speleothems: Elemental incorporation and their potential as environmental archives. *Sedimentology* **66:** 2661–2685. https://doi.org/10.1111/sed.12607

Wadsworth, F.B., Vasseur, J., Casas, A.S., Delmelle, P., Hess, K. (2020) A model for the kinetics of high temperature reactions between polydisperse volcanic ash and SO_2 gas. *In press.*

Watanabe, M., Iwasaka, Y., Shibata, T., Hayashi, M., Fujiwara, M., Neuber, R. (2004) The evolution of Pinatubo aerosols in the Arctic stratosphere during 1994–2000. *Atmospheric Research* **69**: 199–215

Watson, E.J., Kolaczek, P., Slowinski, M., Swindles, G.T., Marcisz, K., Galka, M. Lamentowicz, M. (2017) First discovery of Holocene Alaskan and Icelandic tephra in Polish peatlands. *Journal of Quaternary Science* **32**(4): 457-462

Watson, E.J., Swindles, G.T., Lawson, I.T., Savov, I.P. (2016) Do peatlands or lakes provide the most comprehensive distal tephra records? *Quaternary Science Reviews* **139**: 110–128

Watson, E.J., Swindles, G.T., Lawson, I.T., Savov, I.P. (2015) Spatial variability of tephra and carbon accumulation in a Holocene peatland. *Quaternary Science Reviews* **124**: 248-264

Witham, C.S., Oppenheimer, C., Horwell, C.J. (2005) Volcanic ash-leachates: A review and recommendations for sampling methods. *Journal of Volcanology and Geothermal Research* **141**: 299–326. https://doi.org/10.1016/j.jvolgeores.2004.11.010

Wulf, S. Dräger, N. Ott, F. Serb, J. Appelt, O. Guðmundsdóttir, E. van den Bogaard, C. Slowinski, M. Laszkiewicz, M., Brauder, A. (2016) Holocene tephrostratigraphy of varved sediment records from Lakes Tiefer See (NE Germany) and Czechowskie (N Poland). *Journal of Quaternary Science* **32**: 1-14.

Wynn, P.M., Fairchild, I.J., Borsato, A., Baker, A., Frisia, S. (2013) Biogeochemical cycling of sulphur in the speleothem record. *Biogeochemistry* **114**: 255-267

Zanchettin, D., Bothe, O., Timmreck, C., Bader, J., Beitsch, A., Graf, H.-F., Notz, D., Jungclaus, J.H. (2014) Inter-hemispheric asymmetry in the sea-ice response to volcanic forcing simulated by MPI-ESM (COSMOS-Mill). *Earth System Dynamics* **5**: 223-242

Journal Pre-proof

Zhong, Y., Miller, G. H., Otto-Bliesner, B. L., Holland, M. M., Bailey, D. A., Schneider, D. P., Geirsdottir, A. (2011) Centennial scale climate change from decadally-paced explosive volcanism: a coupled sea ice-ocean mechanism. *Climate Dynamics* **37**: 2373–2387

Zhou, H., Greig, A., Tang, J., You, C. -F., Yuan, D., Tong, X., Huang, Y. (2012) Rare earth element patterns in a Chinese stalagmite controlled by sources and scavenging from karst groundwater. *Geochimica et Cosmochimica Acta* **83**: 1-18

Zhou, H., Wang, Q., Zhao, J., Zheng, L., Guan, H., Feng, Y., Greig, A. (2008a) Rare earth elements and yttrium in a stalagmite from Central China and potential paleoclimatic implications. *Palaeogeography, Palaeoclimatology, Palaeoecology* **270** (1–2): 128–138.

Zhou, H.Y., Chi, B.Q., Lawrence, M., Zhao, J.X., Yan, J., Greig, A., Feng, Y.X. (2008b) High resolution and precisely dated record of weathering and hydrological dynamics recorded by manganese and rare earth elements in a stalagmite from central China. *Quaternary Research* **68:** 438–446

Zielinski, G. A., Mayewski, P. A., Meeker, L. D., Whitlow, S. Twickler, M. S. (1996) A 110,000-yr record of explosive volcanism from the GISP2 (Greenland) ice core. *Quaternary Research* **45**: 109–118

Journal Pre-proof

The trace-element composition of a Polish stalagmite: Implications for the use of speleothems as a record of explosive volcanism

Alice R. Paine[1*], James U. L. Baldini[1], Fabian B. Wadsworth[1], Franziska A. Lechleitner[2], Robert A. Jamieson[3], Lisa M. Baldini[4], Richard J. Brown[1], Wolfgang Müller[5], Helena Hercman[6], Michał Gąsiorowski[6], Krzysztof Stefaniak[7], Paweł Socha[7], Artur Sobczyk[8], Marek Kasprzak[9]

[1] Department of Earth Sciences, Durham University, UK, DH1 3LE

[2] Department of Chemistry and Biochemistry and Oeschger Centre for Climate Change Research, University of Bern, Bern, Switzerland

[3] School of Earth and Environment, University of Leeds, UK

[4] School of Health and Life Sciences, Teesside University, UK

[5] Institut für Geowissenschaften, Goethe Universität, Germany

[6] Institute of Geological Sciences, Polish Academy of Sciences, Poland

[7] Department of Palaeozoology, Zoological Institute, University of Wrocław, Poland

[8] Department of Structural Geology and Geological Mapping, Institute of Geological Sciences, University of Wrocław, Poland

[9] Institute of Geography and Regional Development, University of Wrocław, Poland

*currently at the Department of Earth Sciences, University of Oxford, UK, OX1 3AN (alice.paine@earth.ox.ac.uk)

Journal Pre-proof

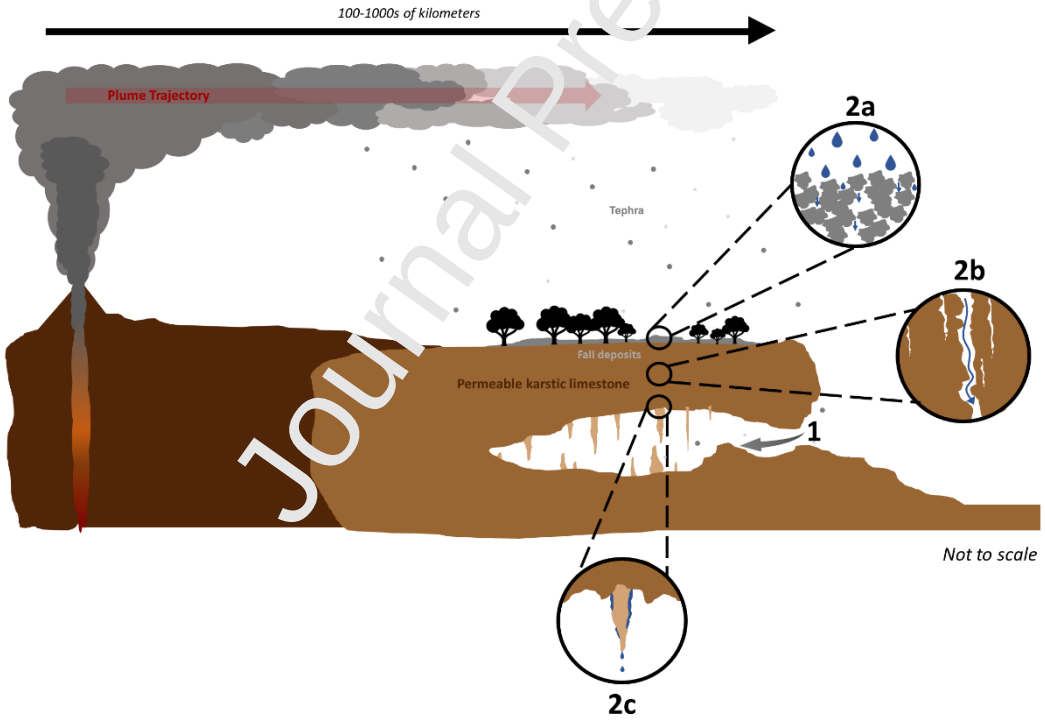

Figure 1. A conceptual diagram illustrating the dominant transport pathways of mass from an eruption to a stalagmite. Pathway 1 is via aeolian transport of ash directly into a cave environment. Pathway 2 is via leaching of tephra and subsequent percolative transport into the cave through the cave roof rock. Insets show specific components of pathway 2. 2a shows leaching of trace elements from fall deposits. 2b shows percolation of leached material in the form of colloids, particulates or solutes through fractures and the permeable karstic limestone. 2c depicts that drip water reaching stalactite tips and dripping onto stalagmite growth surfaces below. This is schematic and not drawn to scale.

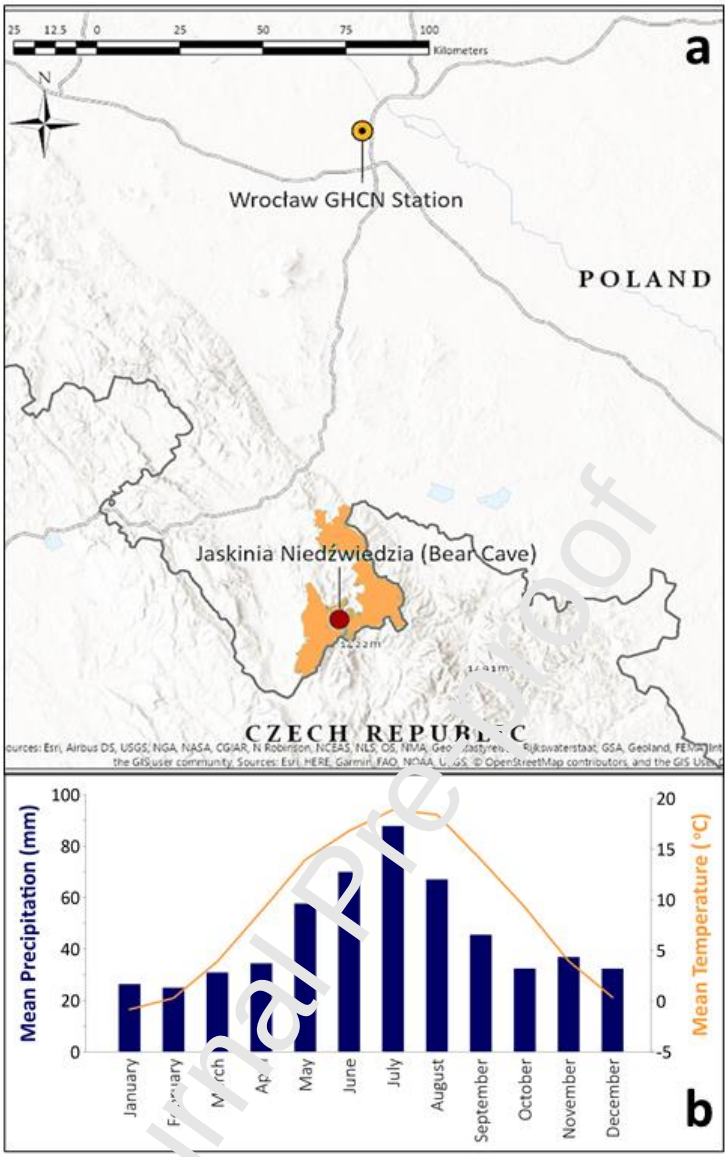

Figure 2. (a) Topographic map of the Niedźwiedzia Cave site within Śnieżnik Landscape Park (orange shading) and location of Wrocław WGHCN station (orange circle). Map created in ArcGIS Pro © (v. 2.4.2.). (b) Wrocław mean monthly temperature (orange line) and precipitation amount (blue bars) for the period 1980-2010 (GHCN Wrocław data). At this central European site, precipitation covaries with temperature with a minimum in winter (between December and March) and maximum in summer (between June and August). Data were obtained from the National Oceanographic and Atmospheric Administration (NOAA)'s Global Historical Climatology Network (GHCN).

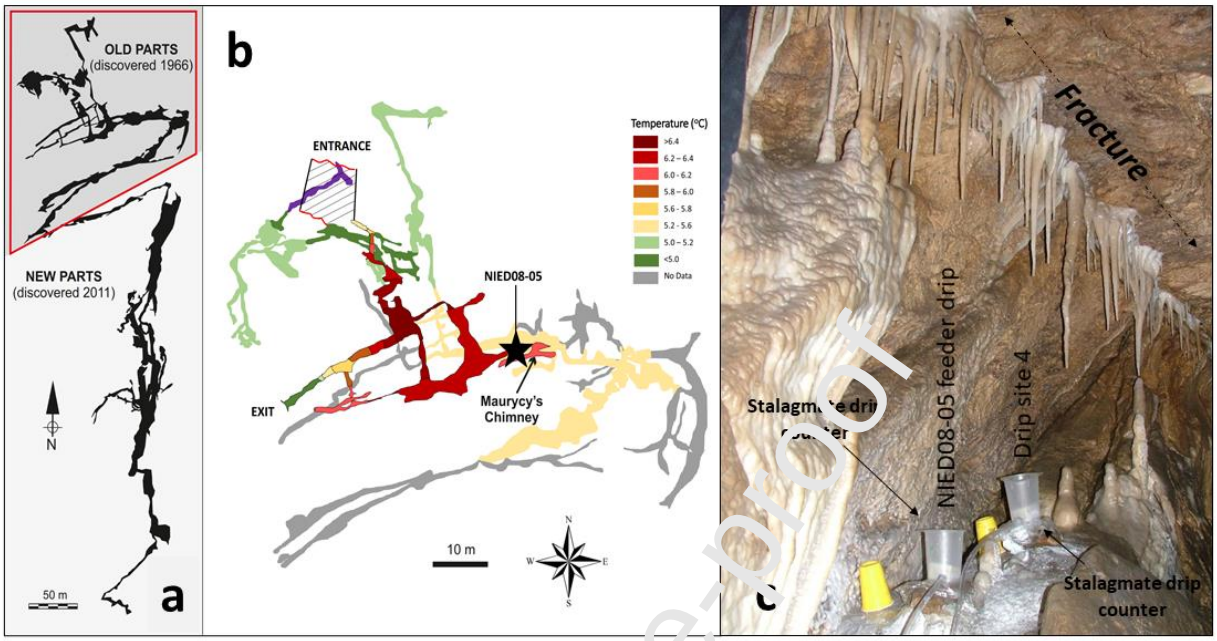

Figure 3. The Niedźwiedzia cave system and sample site. (a) Plan view of the subsurface cave network including "old" and "new" parts and position of analysed area (modified after Kostka 2014); (b) Plan-view diagram of the Niedźwiedzia Cave old parts and Maurycy's Chimney (closest to the surface), depicting mean annual air temperature (colour scale) and the relative location of the NIED08-05 stalagmite (black star). Where the cave map has a black outline, cave portions are in the upper or middle level of the cave (i.e. above the deeper portions that are not given a black outline; map adapted from Lechleitner et al. 2016; temperature data after Piasecki & Sawiński, 2009). (c) Two drip sites: the NIED08-05 feeder drip and drip site 4 (located ~1 m apart along the same fracture) were monitored in Jaskinia Niedźwiedzia, using a Stalagmate drip counter (Collister & Mattey, 2008) between May 2009 and June 2010. Note the well-developed fracture on the ceiling and clear lineation in stalactite and stalagmite deposition.

Journal Pre-proof

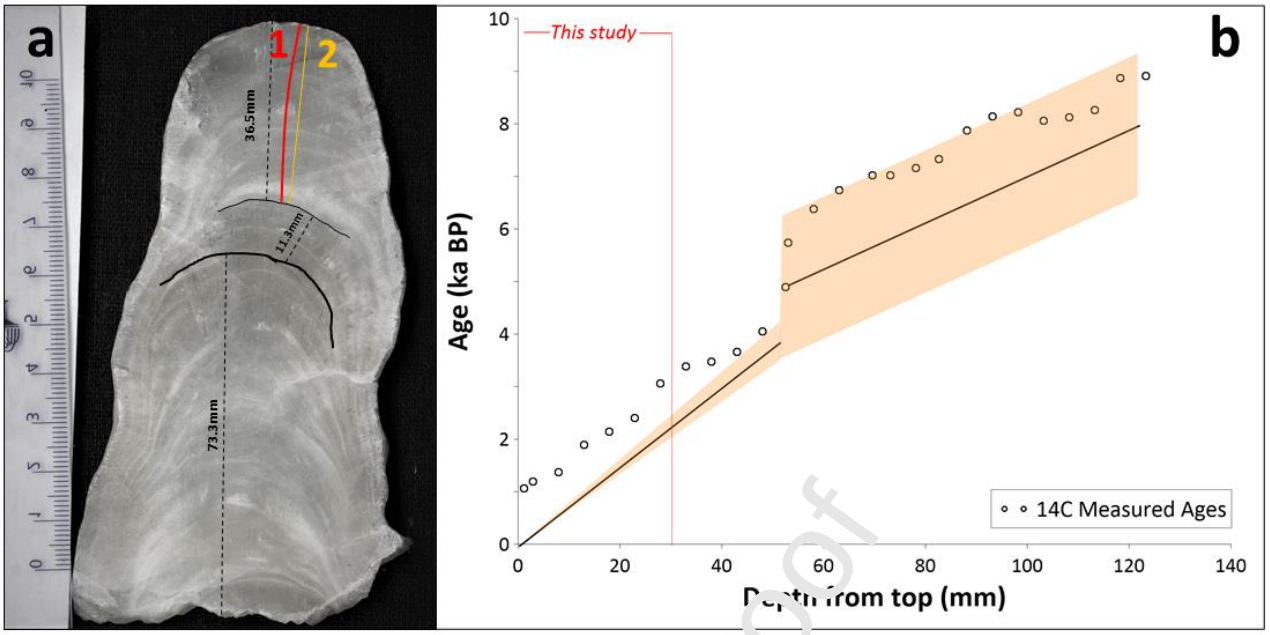

Figure 4: (a) An image of the NIED08-05 stalagmite collected using a binocular microscope (the ruler is numbered in centimeters with individual tick marks for each millimeter). The dashed black lines are used to show the approximate lengths of 3 growth stages and the approximate growth orientation. Laser track 1 (red) and 2 (yellow) are marked. (b) The age-depth chronology for NIED08-05, adapted from Lechleitner et al. (2016) based on ^{14}C dates. Circles show the measured ^{14}C ages with an anchor point given at the 2008 year of sample collection. The black curve shows the best fit age-depth trend based on the corrections and model provided in Lechleitner et al. (2016; details therein). The orange shaded region shows the 95% confidence intervals for the model age-depth trend. Based on the increased errors after the transition from the first to the second growth stage, we restrict our analysis to the portion of the speleothem at <40 mm from the top, equivalent to calculated ages from 0 to 3 ka BP. Note that "top" refers to the top of the stalagmite in panel (a), but is in fact the "bottom" of the stalagmite in terms of the cave environment as collected.

Journal Pre-proof

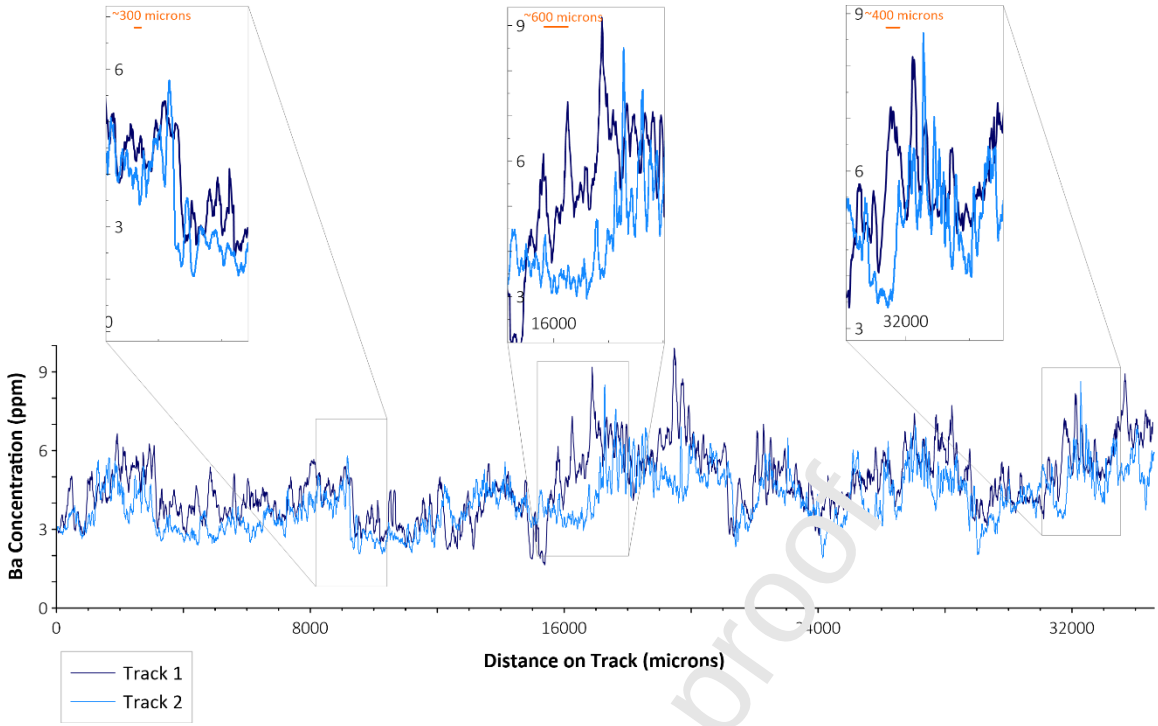

.

Figure 5. A comparison of Ba concentrations measured in track 1 & 2 of stalagmite NIED08-05. Insets show regions in the datasets where a horizontal offset in a common abrupt change can be seen in both datasets. The estimated horizontal magnitude of these offsets is marked in orange and is discussed in the main text. We note that there is broad agreement between the low-frequency trend in track 1 and track 2.

Journal Pre-proof

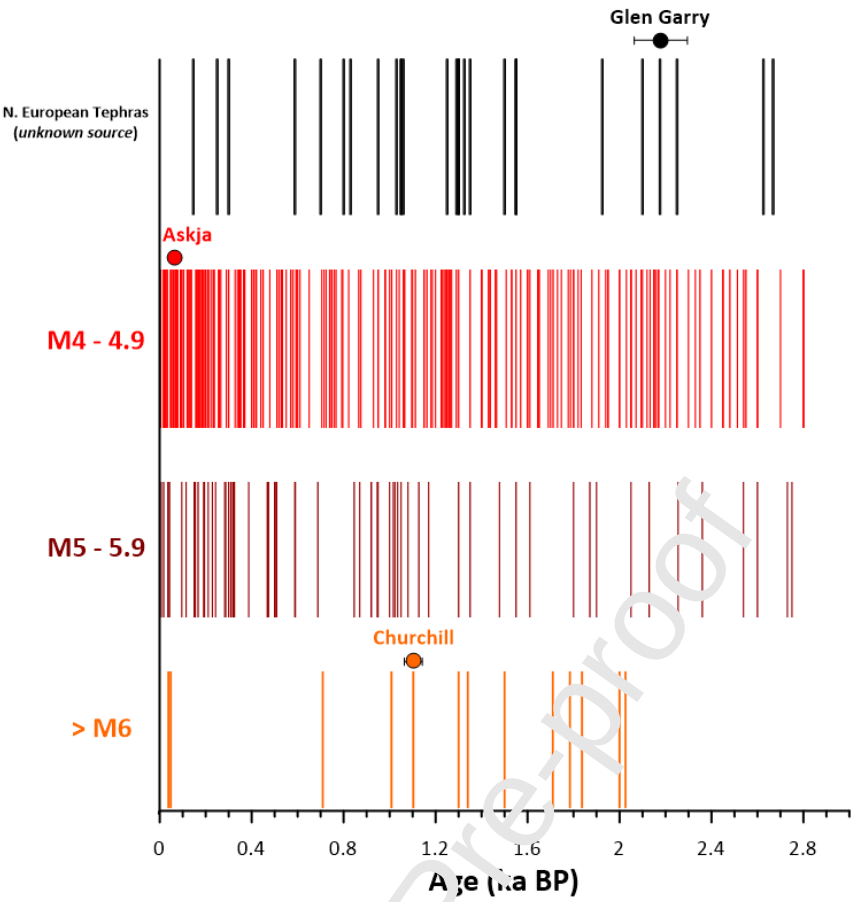

Figure 6: A record of explosive volcanism between 0-3 ka (sourced from LaMEVE), presented by magnitude. Red, orange, and burgundy bars mark individual events. Black bars mark the dates of tephra isochrons yet to be assigned a source eruption (sourced from NEVA) Circles mark the eruptions/isochrons utilised in this study, with dating errors marked by black horizontal lines.

Journal Pre-proof

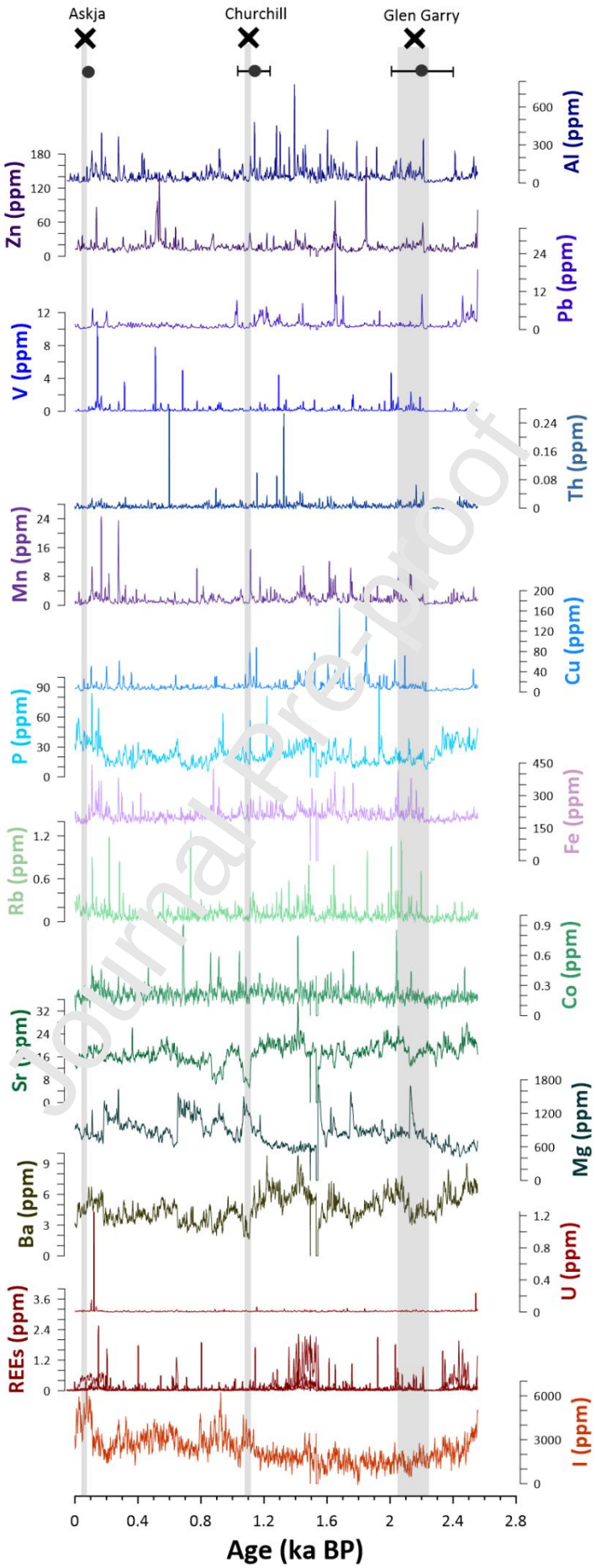

Journal Pre-proof

Figure 7. The raw trace element dataset analysed in this study, and the aggregate of all analysed REEs (where the aggregate is the sum). The absolute NIED08-05 age uncertainties relative to the eruption events discussed in this study are given by the dark grey circles and error-bars (after ^{14}C dates from Lechleitner et al. 2016). The selected eruption events are shown by black crosses at the top, and highlighted in grey are eruption date uncertainties.

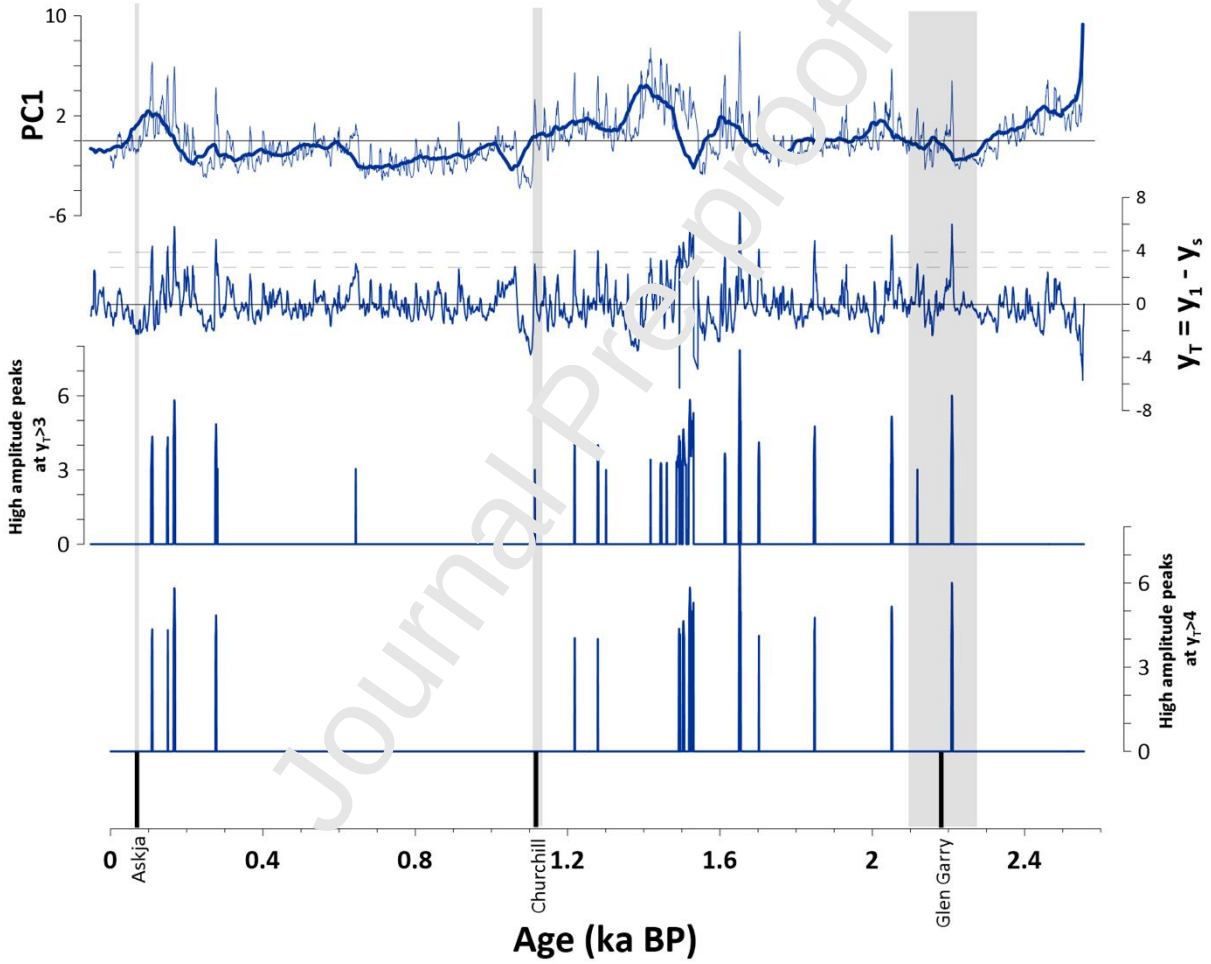

Figure 8. The results of PCA applied to the trace element datasets analysed in NIED08-05 since 3 ka BP. Here we show PC1 (accounting for 17% of the total variability between trace elements) as the blue high resolution curve in (a) along with a low-frequency moving average to these data (thick blue line in (a)) using an averaging window of 75 years, which is larger than the high frequency variability. (b) We define a metric y_T that is the difference between PC1 (termed here y_1) and the low-frequency moving average (termed here y_s), such that $y_T = y_1 - y_s$. This represents a baseline-subtraction to PC1. The dashed line occurs at $y_T = 3$. (c-d) The peaks in PC1 that occur above $y_T = 3$, and $y_T = 4$, respectively. Below we show the eruptions considered in this study (black lines) and the width of the marked grey bars is the dating uncertainty on those eruptions.

Journal Pre-proof

Journal Pre-proof

Journal Pre-proof

Declaration of interests

☒ The authors declare that they have no known competing financial interests or personal relationships that could have appeared to influence the work reported in this paper.

☐The authors declare the following financial interests/personal relationships which may be considered as potential competing interests:

Journal Pre-proof